

Muon Decay

W. Fetscher^{1*}

¹ Institute for Physics and Astrophysics, ETH Zürich

* fetscher@phys.ethz.ch

June 1, 2021



Review of Particle Physics at PSI
doi:[10.21468/SciPostPhysProc.2](https://doi.org/10.21468/SciPostPhysProc.2)

Abstract

The decay of the muon has been studied at PSI with several precision measurements: The longitudinal polarization $P_L(E)$ with the muon decay parameters ξ' , ξ'' , the Time-Reversal Invariance (TRI) conserving transverse polarization $P_{T_1}(E)$ with the muon decay parameters η , η'' , the TRI violating transverse polarization $P_{T_2}(E)$, with α'/A , β'/A and the muon decay asymmetry with $P_\mu \xi$. The detailed theoretical analysis of all measurements of normal and inverse muon decay has led for the first time to a lower limit $|g_{LL}^V| > 0.960$ ("V-A") and upper limits for nine other possible complex couplings, especially the scalar coupling $|g_{LL}^S| < 0.550$ which had not been excluded before.

6.1 Introduction

Muon decay, $\mu^+ \rightarrow \bar{\nu}_\mu e^+ \nu_e$, as a purely leptonic process, provides a precise source of information on the charged current weak interaction. Before the advent of the meson factories LAMPE, TRIUMF and SIN, experimental results were scarce and theoretical descriptions inappropriate to uniquely deduce the interaction. In a combined effort, the ETH-SIN group has performed decisive precision measurements and, simultaneously, developed the theoretical description in a way that allowed the determination of the interaction from experimental results, taken exclusively from normal and inverse muon decay.

6.2 Hamiltonian

The three leptonic decays $\mu^+ \rightarrow \bar{\nu}_\mu e^+ \nu_e$, $\tau^+ \rightarrow \bar{\nu}_\tau \mu^+ \nu_\mu$ and $\tau^+ \rightarrow \bar{\nu}_\tau e^+ \nu_e$, as well as their charge conjugate decays, can be described by the most general, local, derivative-free and lepton-number conserving four-fermion point interaction Hamiltonian. The point interaction allows the use of equivalent Hamiltonians, which differ in the way the fermions are grouped together [1, 2]. The older literature preferred a "charge retention" form with parity-odd and parity-even terms in which e^+ and μ^+ , as the usually detected particles, were grouped together [3, 4]. This had the advantage that limits to some coupling constants could be obtained from then existing results. The disadvantage was that this Hamiltonian represents interactions proceeding via the exchange of a neutral boson X that would carry the lepton numbers both of muon and electron, and so would not be universal. The use of a "charge-changing" form, where the charged leptons are grouped with their neutrinos and which is adapted to charged boson exchange, results in absolute values of differences of coupling constants. Both of these forms are complicated by the fact that a fully parity-violating interaction, such as e.g. the $V-A$ interaction, is represented by four coupling constants C_V , C'_V , C_A and C'_A .

39 In the following, we will use a charge-changing Hamiltonian characterized by fields of
 40 definite handedness [5, 6]. We use the notation of Fetscher *et. al.* [7], who in turn use the sign
 41 conventions and definitions of Scheck [8]. The matrix element is then given by

$$M = 4 \frac{G_F}{\sqrt{2}} \sum_{\substack{\gamma=S,V,T \\ \varepsilon,\mu=R,L}} g_{\varepsilon\mu}^\gamma \langle \bar{e}_\varepsilon | \Gamma^\gamma | (\nu_e)_n \rangle \langle (\bar{\nu}_\mu)_m | \Gamma_\gamma | \mu_\mu \rangle. \quad (6.1)$$

42 Here, G_F is the Fermi coupling constant, while $\gamma = S, V, T$ labels a 4-scalar, 4-vector, or
 43 4-tensor interaction; and $\varepsilon, \mu = R, L$ indicate the chirality (right- or left-handed) of the spinors
 44 of the electron or muon. The chiralities n and m of the ν_e and $\bar{\nu}_\mu$ are then determined by
 45 the values of γ, ε , and μ . In this picture, the coupling constants $g_{\varepsilon\mu}^\gamma$ have a simple physical
 46 interpretation: $n_\gamma |g_{\varepsilon\mu}^\gamma|^2$ is equal to the (relative) probability for a μ -handed muon to decay
 47 into an ε -handed electron by the interaction γ^γ ; the factors $n_S = 1/4$, $n_V = 1$ and $n_T = 3$ take
 48 care of the proper normalisation. The standard model thus corresponds to $g_{LL}^V = 1$, with all
 49 other couplings being zero.

50 We emphasise that here right- and left-handed definitely means chirality and not helicity.
 51 The left-handed spinor $\overset{\circ}{\chi}$ of a fermion in its rest system transforms under a Lorentz-boost as

$$\chi_L(\mathbf{p}) = \frac{(E+m)\sigma^0 - \mathbf{p} \cdot \boldsymbol{\sigma}}{\sqrt{2m(E+m)}} \overset{\circ}{\chi}, \quad (6.2)$$

52 where σ^0 and $\boldsymbol{\sigma}$ are the four Pauli matrices. By a parity operation, $\chi_L(\mathbf{p})$ becomes the right-
 53 handed spinor $\chi_R(\mathbf{p})$. Left- and right-handed spinors are contained in separate $\mathbb{C}2$ -spaces.
 54 The right-handed spinor transforms under a Lorentz-boost as

$$\chi_R(\mathbf{p}) = \frac{(E+m)\sigma^0 + \mathbf{p} \cdot \boldsymbol{\sigma}}{\sqrt{2m(E+m)}} \overset{\circ}{\chi}. \quad (6.3)$$

55 The spinor of the antiparticle is given by

$$\varphi_L(\mathbf{p}) = +i\sigma^2 \chi_R^*(\mathbf{p}) \quad \text{and} \quad \varphi_R(\mathbf{p}) = -i\sigma^2 \chi_L^*(\mathbf{p}) \quad (6.4)$$

56 6.3 Observables

57 The differential decay probability to obtain an e^\pm with (reduced) energy between x and $x+dx$,
 58 emitted in the direction $\hat{\mathbf{x}}_3$ at an angle between ϑ and $\vartheta+d\vartheta$ with respect to the muon polar-
 59 ization vector \mathbf{P}_μ , and with its spin parallel to the arbitrary direction $\hat{\boldsymbol{\zeta}}$, neglecting radiative
 60 corrections, is given by

$$\frac{d^2\Gamma}{dx d\cos\vartheta} = \frac{m_\mu}{4\pi^3} W_{e\mu}^4 G_F^2 \sqrt{x^2 - x_0^2} \cdot \{F_{IS}(x) \pm P_\mu \cos\vartheta F_{AS}(x)\} \cdot \{1 + \hat{\boldsymbol{\zeta}} \cdot \mathbf{P}_e(x, \vartheta)\} \quad (6.5)$$

61 Here, $W_{e\mu} = \max(E_e) = (m_\mu^2 + m_e^2)/(2m_\mu)$ is the maximum e^\pm energy, $x = E_e/W_{e\mu}$ is the re-
 62 duced energy, $x_0 = m_e/W_{e\mu} = 9.67 \times 10^{-3}$, and $P_\mu = |\mathbf{P}_\mu|$ is the degree of muon polarization.
 63 $\hat{\boldsymbol{\zeta}}$ is the direction in which a perfect polarization-sensitive electron detector is most sensitive.
 64 The isotropic part of the spectrum, $F_{IS}(x)$, the anisotropic part $F_{AS}(x)$, and the electron po-
 65 larization, $\mathbf{P}_e(x, \vartheta)$, may be parameterized by the Michel parameter ρ [1], by η [9], by ξ and
 66 δ [3, 10], *etc.* These are bilinear combinations of the coupling constants $g_{\varepsilon\mu}^\gamma$, which occur in
 67 the matrix element (given below).

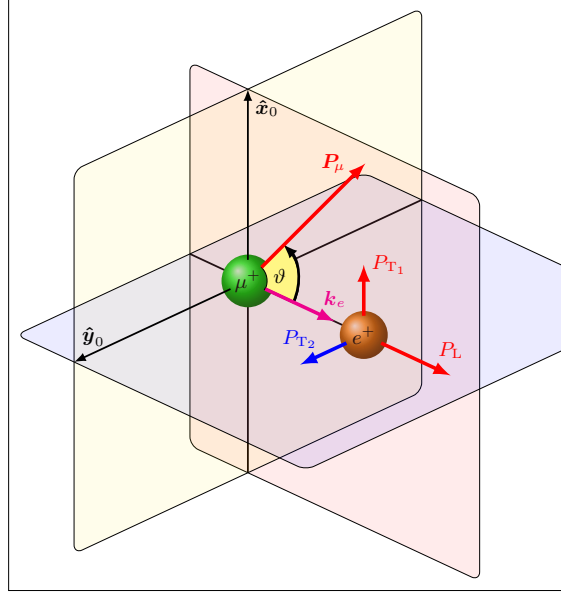


Figure 6.1: Definition of the observables in polarized muon decay: muon polarization \mathbf{P}_μ , positron momentum \mathbf{k}_e , longitudinal positron polarization P_L , transverse positron polarization (P_{T_1} , P_{T_2}) and angle of emission ϑ (relative to \mathbf{P}_μ). Time reversal invariance is violated if $P_{T_2} \neq 0$. From [11].

68 If the masses of the neutrinos as well as x_0 are neglected, the energy and angular distri-
 69 bution of the electron in the rest frame of a muon (μ^\pm) measured by a polarization insensitive
 70 detector is given by

$$\frac{d^2\Gamma}{dx d\cos\vartheta} \sim x^2 \cdot \left\{ 3(1-x) + \frac{2\rho}{3}(4x-3) + 3\eta x_0(1-x)/x \right. \\ \left. \pm P_\mu \cdot \xi \cdot \cos\vartheta \left[1-x + \frac{2\delta}{3}(4x-3) \right] \right\} \quad (6.6)$$

71 Here, ϑ is the angle between the electron momentum and the muon spin, and $x \equiv 2E_e/m_\mu$.
 72 For the Standard-Model coupling, we obtain $\rho = \xi\delta = 3/4$, $\xi = 1$, $\eta = 0$ and the differential
 73 decay rate is

$$\frac{d^2\Gamma}{dx d\cos\vartheta} = \frac{G_F^2 m_\mu^5}{192\pi^3} [3 - 2x \pm P_\mu \cos\vartheta(2x-1)] x^2 \quad (6.7)$$

74 The coefficient in front of the square bracket is the total decay rate.

75 The observables in the decay of polarized muons are shown in Figure 6.1. We have defined
 76 a right-handed coordinate system with

$$\hat{\mathbf{z}} = \frac{\mathbf{k}_e}{|\mathbf{k}_e|}, \quad \hat{\mathbf{y}} = \frac{\mathbf{k}_e \times \mathbf{P}_\mu}{|\mathbf{k}_e \times \mathbf{P}_\mu|}, \quad \hat{\mathbf{x}} = \hat{\mathbf{y}} \times \hat{\mathbf{z}} \quad (6.8)$$

77 Here, \mathbf{k}_e is the momentum vector of the electron, while P_L designates the longitudinal po-
 78 larization, P_{T_1} the transverse component of \mathbf{P}_e lying in the plane defined by \mathbf{k}_e and \mathbf{P}_μ , and
 79 P_{T_2} is the component perpendicular to that plane. $P_{T_2} \neq 0$ signals violation of time-reversal

80 symmetry. These polarization components are

$$P_{T_1}(x, \vartheta) = \frac{P_\mu \sin \vartheta \cdot F_{T_1}(x)}{F_{IS}(x) \pm P_\mu \cos \vartheta \cdot F_{AS}(x)} \quad (6.9)$$

$$P_{T_2}(x, \vartheta) = \frac{P_\mu \sin \vartheta \cdot F_{T_2}(x)}{F_{IS}(x) \pm P_\mu \cos \vartheta \cdot F_{AS}(x)} \quad (6.10)$$

$$P_L(x, \vartheta) = \frac{\pm F_{IP}(x) + P_\mu \cos \vartheta \cdot F_{AP}(x)}{F_{IS}(x) \pm P_\mu \cos \vartheta \cdot F_{AS}(x)}. \quad (6.11)$$

81 If only the neutrino masses are neglected, and if the e^\pm polarization is detected, then the
82 functions in (6.5) can be decomposed as [12]

$$F_\nu(x) = F_\nu^{V-A}(x) + G_\nu(x), \quad (6.12)$$

83 where $G_\nu(x) \equiv 0$ for $g_{LL}^V = 1$ ("V - A"). Physics beyond the Standard Model would thus be
84 contained *exclusively* in the $G_\nu(x)$. The index ν stands for IS (isotropic part of the spectrum),
85 AS (anisotropic part of the spectrum), T_1 (transverse polarization P_{T_1}), T_2 (transverse polar-
86 ization P_{T_2}), IP (isotropic part of the longitudinal polarization) and AP (anisotropic part of the
87 longitudinal polarization). The $F_\nu^{V-A}(x)$ do not depend on specific decay parameters:

$$F_{IS}^{V-A}(x) = \frac{1}{6} \{-2x^2 + 3x - x_0^2\} \quad (6.13a)$$

$$F_{AS}^{V-A}(x) = \frac{1}{6} (x^2 - x_0^2)^{1/2} \{2x - 2 + (1 - x_0^2)^{1/2}\} \quad (6.13b)$$

$$F_{T_1}^{V-A}(x) = -\frac{1}{6} / (1 - x)x_0 \quad (6.13c)$$

$$F_{T_2}^{V-A}(x) = 0 \quad (6.13d)$$

$$F_{IP}^{V-A}(x) = \frac{1}{6} (x^2 - x_0^2)^{1/2} \{-2x + 2 + (1 - x_0^2)^{1/2}\} \quad (6.13e)$$

$$F_{AP}^{V-A}(x) = \frac{1}{6} \{-2x^2 - x - x_0^2\} \quad (6.13f)$$

88 The functions $G_\nu(x)$ depend on the decay parameters $\rho, \xi'', \xi', \xi, \delta, \eta, \eta'', \alpha'/A, \beta'/A$, where
89 $\eta = (\alpha - 2\beta)/A$ and $\eta'' = (3\alpha + 2\beta)/A$:

$$G_{IS}(x) = \frac{1}{9} \{2(\rho - \frac{3}{4})(4x^2 - 3x - x_0^2) + 9\eta(1 - x)x_0\} \quad (6.14a)$$

$$G_{AS}(x) = \frac{1}{9} (x^2 - x_0^2)^{1/2} \{3(\xi - 1)(1 - x) + 2(\xi\delta - \frac{3}{4})(4x - 4 + (1 - x_0^2)^{1/2})\} \quad (6.14b)$$

$$G_{T_1}(x) = \frac{1}{12} \left\{ -2 \left[(\xi'' - 1) + 12 \left(\rho - \frac{3}{4} \right) \right] (1 - x)x_0 - 3\eta(x^2 - x_0^2) + \eta''(-3x^2 + 4x - x_0^2) \right\} \quad (6.14c)$$

$$G_{T_2}(x) = \frac{1}{3} (x^2 - x_0^2)^{1/2} \left\{ 3 \frac{\alpha'}{A} (1 - x) + 2 \frac{\beta'}{A} (1 - x_0^2)^{1/2} \right\} \quad (6.14d)$$

$$G_{IP}(x) = \frac{1}{54} (x^2 - x_0^2)^{1/2} \left\{ 9(\xi' - 1) \left[-2x + 2 + (1 - x_0^2)^{1/2} \right] + 4\xi \left(\delta - \frac{3}{4} \right) \left[4x - 4 + (1 - x_0^2)^{1/2} \right] \right\} \quad (6.14e)$$

$$G_{AP}(x) = \frac{1}{6} \left\{ (\xi'' - 1)(2a^2 - x - x_0^2) + 4(\rho - \frac{3}{4})(4x^2 - 3x - x_0^2) + 2\eta''(1 - x)x_0 \right\} \quad (6.14f)$$

90 Several of the decay parameters $\{\rho, \xi, \xi', \xi'', \delta, \eta, \eta'', \alpha/A, \beta/A, \alpha'/A, \beta'/A\}$, which are not
91 all independent, have been measured in the past. Past experiments have also been analyzed

92 using the parameters $a, b, c, a', b', c', \alpha/A, \beta/A, \alpha'/A, \beta'/A$ (and $\eta = (\alpha - 2\beta)/2A$), as defined
 93 by Kinoshita and Sirlin [3, 10]. They serve as a model-independent summary of all possible
 94 measurements on the decay electron (see Listings below). The relations between the two sets
 95 of parameters are

$$\rho - \frac{3}{4} = \frac{3}{4}(-a + 2c)/A \quad (6.15)$$

$$\eta = (\alpha - 2\beta)/A \quad (6.16)$$

$$\eta'' = (3\alpha + 2\beta)/A \quad (6.17)$$

$$\delta - \frac{3}{4} = \frac{9}{4} \frac{(a' - 2c')/A}{1 - [a + 3a' + 4(b + b') + 6c - 14c']/A} \quad (6.18)$$

$$1 - \xi \frac{\delta}{\rho} = 4 \frac{[(b + b') + 2(c - c')]/A}{1 - (a - 2c)/A} \quad (6.19)$$

$$1 - \xi' = [(a + a') + 4(b + b') + 6(c + c')]/A \quad (6.20)$$

$$1 - \xi'' = (-2a + 20c)/A \quad (6.21)$$

96 where

$$A = a + 4b + 6c \quad (6.22)$$

97 The ten complex amplitudes $g_{\varepsilon\mu}^\gamma$ (g_{RR}^T and g_{LL}^T are identically zero) and G_F constitute 20 inde-
 98 pendent (real) parameters to be determined by experiment. The Standard Model interaction
 99 corresponds to one single amplitude g_{LL}^V being unity and all the others being zero.

100 6.4 Lorentz Structure

101 The nine parameters $\{\rho, \xi, \xi', \xi'', \delta, \eta, \eta'', \alpha'/A, \beta'/A\}$ describing the electron spectrum,
 102 decay asymmetry and polarization vector can be represented [3] by the intermediate quantities
 103 $\{a, a', \alpha, \alpha', b, b', \beta, \beta', c, c'\}$, whose values are known from experiment [13]. They are all
 104 real, bilinear combinations of the coupling constants:

$$a = 16(|g_{RL}^V|^2 + |g_{LR}^V|^2) + |g_{RL}^S + 6g_{RL}^T|^2 + |g_{LR}^S + 6g_{LR}^T|^2 \quad (6.23a)$$

$$a' = 16(|g_{RL}^V|^2 - |g_{LR}^V|^2) + |g_{RL}^S + 6g_{RL}^T|^2 - |g_{LR}^S + 6g_{LR}^T|^2 \quad (6.23b)$$

$$\alpha = 8\text{Re}\{g_{LR}^V(g_{RL}^{S*} + 6g_{RL}^{T*}) + g_{RL}^V(g_{LR}^{S*} + 6g_{LR}^{T*})\} \quad (6.23c)$$

$$\alpha' = 8\text{Im}\{g_{LR}^V(g_{RL}^{S*} + 6g_{RL}^{T*}) - g_{RL}^V(g_{LR}^{S*} + 6g_{LR}^{T*})\} \quad (6.23d)$$

$$b = 4(|g_{RR}^V|^2 + |g_{LL}^V|^2) + |g_{RR}^S|^2 + |g_{LL}^S|^2 \quad (6.23e)$$

$$b' = 4(|g_{RR}^V|^2 - |g_{LL}^V|^2) + |g_{RR}^S|^2 - |g_{LL}^S|^2 \quad (6.23f)$$

$$\beta = -4\text{Re}\{g_{RR}^V g_{LL}^{S*} + g_{LL}^V g_{RR}^{S*}\} \quad (6.23g)$$

$$\beta' = 4\text{Im}\{g_{RR}^V g_{LL}^{S*} - g_{LL}^V g_{RR}^{S*}\} \quad (6.23h)$$

$$c = \frac{1}{2}\{|g_{RL}^S - 2g_{RL}^T|^2 + |g_{LR}^S - 2g_{LR}^T|^2\} \quad (6.23i)$$

$$c' = \frac{1}{2}\{|g_{RL}^S - 2g_{RL}^T|^2 - |g_{LR}^S - 2g_{LR}^T|^2\} \quad (6.23j)$$

105 From (6.23a) to (6.23j) it can be seen that these quantities are not completely independent.
 106 The transformation from the 20-dimensional space of the complex $g_{\varepsilon\mu}^\gamma$ to the 10-dimensional
 107 space of the $\{a, \dots, c'\}$ leads to the following constraints [14]:

$$a \geq 0 \quad a^2 \geq a'^2 + \alpha^2 + \alpha'^2 \quad (6.24)$$

$$b \geq 0 \quad b^2 \geq b'^2 + \beta^2 + \beta'^2 \quad (6.25)$$

$$c \geq 0 \quad c^2 \geq c'^2 \quad (6.26)$$

108 These constraints are very important for any general analysis of muon decay, as they strongly
 109 influence the final errors of the quantities they relate.

110 The precise measurement of individual decay parameters alone generally does not give
 111 conclusive information about the decay interaction due to the many different couplings and
 112 the interference terms between them. A good example for this is the famous Michel parameter
 113 ϱ . A precise measurement yielding the $V - A$ value of $3/4$ by no means establishes the $V - A$
 114 interaction. In fact any interaction consisting of an arbitrary combination of g_{LL}^S , g_{LR}^S , g_{RL}^S ,
 115 g_{RR}^S , g_{RR}^V and g_{LL}^V will yield exactly $\varrho = \frac{3}{4}$. This can be seen if we write ϱ in the form [15]

$$\varrho - \frac{3}{4} = -\frac{3}{4}\{|g_{LR}^V|^2 + |g_{RL}^V|^2 + 2(|g_{LR}^T|^2 + |g_{RL}^T|^2) - \text{Re}(g_{LR}^S g_{LR}^{T*} + g_{RL}^S g_{RL}^{T*})\} \quad (6.27)$$

116 For $\varrho = 3/4$ and $g_{LR}^T = g_{RL}^T = 0$ (no tensor interaction) we find $g_{LR}^V = g_{RL}^V = 0$, with all the
 117 remaining six couplings being arbitrary!

118 The magnitude of the decay interaction is contained in the Fermi coupling constant G_F .
 119 Thus the $g_{\mu\nu}^\gamma$ may be normalized, dimensionless coupling constants, resulting in

$$A \equiv a + 4b + 6c = 16 \quad (6.28)$$

120 This is equivalent to

$$Q_{RR} + Q_{LR} + Q_{RL} + Q_{LL} = 1, \quad (6.29)$$

121 where

$$Q_{RR} = \frac{1}{4}|g_{RR}^S|^2 + |g_{RR}^V|^2 \quad (6.30)$$

$$Q_{RL} = \frac{1}{4}|g_{RL}^S|^2 + |g_{RL}^V|^2 + 3|g_{RL}^T|^2 \quad (6.31)$$

$$Q_{LR} = \frac{1}{4}|g_{LR}^S|^2 + |g_{LR}^V|^2 + 3|g_{LR}^T|^2 \quad (6.32)$$

$$Q_{LL} = \frac{1}{4}|g_{LL}^S|^2 + |g_{LL}^V|^2 \quad (6.33)$$

122 We note that $0 \leq Q_{\varepsilon\mu} \leq 1$ and $\sum_{\varepsilon\mu} Q_{\varepsilon\mu} = 1$. $Q_{\varepsilon\mu}$ is then the probability for the decay of a
 123 muon of handedness μ into an electron of handedness ε . The main point is now that the $Q_{\varepsilon\mu}$
 124 can be expressed by the known quantities $\{a, \dots, c'\}$ [7]:

$$Q_{RR} = 2(b + b')/A \quad (6.34)$$

$$Q_{RL} = [(a - a') + 6(c - c')]/(2A) \quad (6.35)$$

$$Q_{LR} = [(a + a') + 6(c + c')]/(2A) \quad (6.36)$$

$$Q_{LL} = 2(b - b')/A \quad (6.37)$$

125 In the Standard Model, $Q_{LL} = 1$ and the others are zero. The existing measurements show
 126 that the three probabilities Q_{RR} , Q_{LR} and Q_{LL} are zero, within errors. This gives upper limits to
 127 the absolute values of eight of the ten complex coupling constants. Furthermore, we find that
 128 Q_{LL} is bounded by a lower limit which shows that both muon and electron are left-handed. It
 129 can be seen from (6.33), however, that the data from the measurements of the muon and the
 130 electron do not allow one to distinguish a vector (g_{LL}^V) from a scalar (g_{LL}^S) interaction. This
 131 type of ambiguity has been noted before in the context of a different Hamiltonian [16, 17] and
 132 electron-neutrino correlation measurements (not performed up to date) have been proposed.
 133 The total rate S , normalized to the rate predicted by $V - A$ for the reaction $\nu_\mu + e^- \rightarrow \mu^- + \nu_e$
 134 with ν_μ of negative helicity, has been found to be close to 1 [17, 18]. S effectively depends
 135 only on those five coupling constants g_{LL}^V , g_{RL}^V , g_{LR}^S , g_{LR}^T and g_{RR}^S that describe interactions with
 136 left-handed ν_μ . The four latter coupling constants are found to be small. One thus obtains [7]

$$S = |g_{LL}^V|^2 \quad (6.38)$$

137 which yields a *lower* limit for $|g_{LL}^V|$, and through the normalisation requirement (6.29) an
 138 upper limit for the remaining $|g_{LL}^S|$:

$$|g_{LL}^S| < 2\sqrt{1-S} \quad (6.39)$$

139 Thus the weak interaction has been completely determined for muon decay using only data
 140 from this purely leptonic interaction.

141 6.5 Experiments

142 6.5.1 Longitudinal Positron Polarization

143 The measurement of the longitudinal polarization P_L of the electrons from the decay of po-
 144 larized or unpolarized muons allows the determination of the parameters ξ' and ξ'' , as can
 145 be seen from (6.11), (6.12), (6.14e) and (6.14f). The parameter ξ' is of special interest. In
 146 terms of the coupling constants $g_{\varepsilon\mu}^Y$ we have

$$\begin{aligned} 1 - \xi' &= \frac{1}{2} \{4 \cdot (|g_{RR}^V|^2 + |g_{RL}^V|^2) + (|g_{RR}^S|^2 + |g_{RL}^S|^2) + 12 \cdot |g_{RL}^T|^2\} \\ &= 2(Q_{RR} + Q_{RL}) \equiv 2Q_R^e, \end{aligned} \quad (6.40)$$

147 where Q_R^e is the probability of the decay of a muon with chirality μ into an electron with
 148 chirality ε . Note that (6.40) is a sum of absolute squares where only coupling constants with
 149 $\varepsilon = R$ appear. A deviation of ξ' from 1 would require the existence of a coupling with the right-
 150 handed components of the electron, i.e. at least one $g_{R\mu}^Y \neq 0$. Conversely, a measurement with
 151 the result $\xi' = 1$ would prove that the coupling acts exclusively on the left-handed component
 152 of the electron.

153 To determine ξ' , the longitudinal polarization P_L of the electrons from unpolarized muons
 154 has been measured. For the purpose of illustration, we neglect the electron mass m_e and use
 155 the experimentally well confirmed values $\varrho = \delta = \frac{3}{4}$ and obtain from (6.11)

$$\xi' = P_L \quad (6.41)$$

156 The measurement of the electron's longitudinal polarization P_L consists of a comparison with
 157 the spin polarization of the electrons contained in a piece of saturated ferromagnetic material
 158 [19–21]. The comparison is done by scattering the decay electrons from the electrons of a
 159 ferromagnet, using the fact that relativistic electron-electron scattering most often occurs when
 160 the two spins have opposite directions.

161 The experiment was performed at the $\pi E1$ beam line at SIN. A schematic view of the appa-
 162 ratus is shown in Figure 6.2. The 150-MeV/c π^+ beam was stopped in an oak target, where the
 163 π^+ decay resulted in an unpolarized sample of μ^+ within the oak target. Positrons from muon
 164 decay crossed a magnetised iron foil, where they could annihilate in flight with polarized elec-
 165 trons (ANN), $e^+e^- \rightarrow \gamma\gamma$, or scatter elastically: Bhabha-scattering BHA), $e^+e^- \rightarrow e^+e^-$. Both
 166 reactions have high analysing powers up to 90%. The electron polarization in the iron foil
 167 was $(54.44 \pm 0.56) \times 10^{-3}$. The final result of this experiment is [14]

$$\langle |P_L| \rangle = 0.998 \pm 0.042 \quad (6.42)$$

168 From the resulting error of ξ' , which is dominated by the error of $\langle |P_L| \rangle$, upper limits for all
 169 couplings of right-handed electrons to muons (of any handedness) $g_{R\mu}^Y, \mu = R, L$, follow, in
 170 principle, from (6.40). Improved values of these limits are obtained for $|g_{RL}^V|$ and $|g_{RL}^S + 6g_{RL}^T|$
 171 by also considering

$$B_{RL} = \frac{1}{16}|g_{RL}^S + 6g_{RL}^T|^2 + |g_{RL}^V|^2 = \frac{1}{2A}(a + a') \quad (6.43)$$

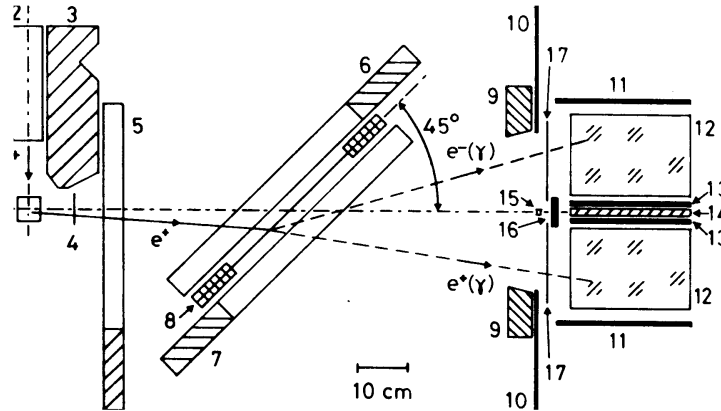


Figure 6.2: Schematic top view of the apparatus used for the measurement of P_L . A typical event is shown for either ANN or BHA. The experimental arrangement: (1) oak stopping target; (2) Be-CH₂ moderator; (3) shielding; (4) timing counter; (5), (6), and (7) multiwire proportional chambers labeled in the text WC₁, WC₂, and WC₃, respectively; and (8) magnet with iron foil. The total-absorption spectrometer is symmetric to the central axis. It consists of (12) four NaI detectors (only the upper pair is shown); (9) square Pb collimator; (10) square-aperture anticoincidence counter; (15) Am-Be calibration source; (17) four electron-identification counters; (16) vertical anticoincidence counter and monitor; (11) and (13) vertical anticoincidence counters; (14) vertical Fe-Pb photon converters. Not shown are the horizontal counterparts of (11), (13), (14) and (16).

172 The parameter ξ'' in μ^+ decay has been determined from a measurement of $P_L(x, \vartheta)$ as
 173 a function of the reduced energy x and the angle ϑ between the muon spin and the positron
 174 momentum [14]. The precision of the measured combination $(\xi'' - \xi\xi')/\xi = -0.35 \pm 0.33$
 175 does, however, not lead to better constraints of the couplings. With a new dedicated setup this
 176 value was considerably improved to [22]

$$\xi'' = 0.981 \pm 0.045_{\text{stat.}} \pm 0.003_{\text{sys.}} \quad (6.44)$$

177 6.5.2 Transverse Positron Polarization

178 Transverse electron polarization $\mathbf{P}_T = (P_{T_1}, P_{T_2})$ is defined in Figure 6.1 and (6.9) and (6.10).
 179 Independent of any assumption about the mechanism of muon decay or even the nature of the
 180 two unobserved neutral particles, time reversal invariance (disregarding the negligible final
 181 state interactions) requires $P_{T_2} = 0$.

182 The measurement of \mathbf{P}_T as a function of energy yields a determination of the parameters
 183 η , η'' , α/A and α'/A (see (6.16), (6.17), (6.23d) and (6.23h)). η is of special interest. η ,
 184 together with the Michel parameter ρ , determines the shape of the (isotropic) positron energy
 185 spectrum. However, it is difficult to deduce its value from a spectrum measurement, as its
 186 influence is suppressed by a factor $x_0 \approx 10^{-2}$. On the other hand, a precise value is needed
 187 for a precise determination of ρ , as η and ρ are statistically highly correlated. In (6.14c) for
 188 P_{T_1} , η arises without a suppression factor. It is interesting to note that P_{T_1} does not vanish in
 189 the Standard Model interaction, as can be seen from (6.9), and it may take sizeable values
 190 ($|P_{T_1}| \leq 1/3$) for positron energies of a few MeV.

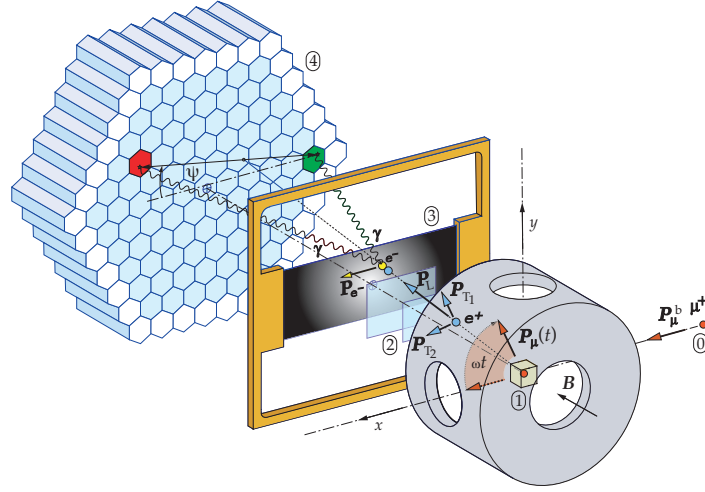


Figure 6.3: Schematic view of the experimental setup for the measurement of P_T . **0**: Burst of polarized muons (angular frequency ω , polarization P_μ^b). **1**: Be stop target and precession field B . **2**: Two plastic scintillation counters selecting decay positrons **3**: Magnetized Vacoflux 50TM foil serving as a polarization analyzer. **4**: Array of 127 BGO scintillators to detect the two γ 's from e^+ annihilation-in-flight. From [23].

191 The experiment was performed with basically the same setup used for measuring the longi-
 192 tudinal polarization. It also uses a comparison with the spin polarized electrons in a ferromag-
 193 netic foil from annihilation in flight $e^+e^- \rightarrow \gamma\gamma$. It is based on the fact that the photons from
 194 the annihilation of a relativistic, transversely polarized positron electron pair are preferentially
 195 emitted in the plane defined by the particle line-of-flight \mathbf{k}_{e^+} and the bisector \mathbf{b} between the
 196 (transverse) polarization directions \mathbf{p}_T and \mathbf{p}_{e^-} .

197 The results of a general, unrestricted analysis of the data are an improved value for
 198 $\eta = (11 \pm 85) \times 10^{-3}$ and the first results for $\eta'' = (48 \pm 125) \times 10^{-3}$ and the T-violating
 199 parameters $\alpha' = (-47 \pm 52) \times 10^{-3}$ and $\beta' = (17 \pm 18) \times 10^{-3}$ [13].

200 An improved experiment, where all the major parts of the previous experiment have been
 201 replaced by newly designed equipment to increase the event rate and reduce the systematic
 202 errors, has been described in detail elsewhere [25]. The four NaI detectors were replaced by an
 203 array of 127 BGO detectors (see Figure 6.3). A longitudinally polarized μ^+ beam ($P_\mu^b = 91\%$)
 204 enters a beryllium stop target with bunches every 19.75 ns. The polarization $P_\mu(t)$ of the
 205 stopped muons precesses in a homogeneous magnetic field ($B = 373.6 \pm 0.4$ mT) with the
 206 same angular frequency ω as the accelerator radio frequency. This ensures that $P_\mu(t) \parallel P_\mu^b$ for
 207 each newly arriving μ^+ bunch. Because of the burst width of 3.9 ns (FWHM) the polarization
 208 $P_\mu(0)$ of the stopped μ^+ is reduced to $(82 \pm 2)\%$. A system of drift chambers (not shown) and
 209 two thin plastic scintillator counters T_0 and T_1 select decay e^+ 's emitted in the direction of B .
 210 A 1-mm-thick magnetized Vacoflux 50TM foil (49% Fe, 49% Co, 2%V) in the central region
 211 with its polarized e^- are selected by an array of 91 interior $\text{Bi}_4\text{Ge}_3\text{O}_{12}$ (BGO) crystals with
 212 plastic veto counters in front of them to reject charged particles. The outer layer of 36 BGOs
 213 assists in an efficient collection of the deposited energy. Valid events are selected by using
 214 the correlation between the γ energies and their opening angle. The intensity distribution
 215 of the two γ 's has roughly the shape of the figure eight with a maximum in the direction of
 216 the bisector of $\mathbf{P}_T(t)$ and the e^- polarization \mathbf{P}_{e^-} [11, 24]. The precession of $\mathbf{P}_\mu(t)$ implies a
 217 precession of $\mathbf{P}_T(t)$, while \mathbf{P}_{e^-} remains constant in time. Thus the intensity distribution of the
 218 γ 's also precesses with frequency ω . For any given pair ij of BGO detectors we ideally expect

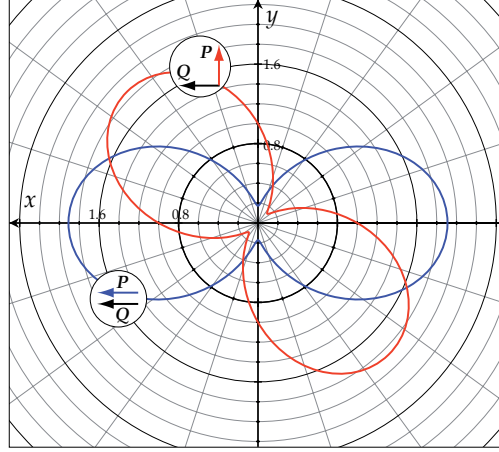


Figure 6.4: Intensity distributions of the annihilation photons at $E_3 = E_4 = 50 m_e$ for parallel spins ($e^- : Q = 1, e^+ : P_T = 1$) and for perpendicular spins. The maximum of the intensity lies on the bisector of the angle ωt between the two spins. Thus the “figure of eight” moves with angular frequency $\omega/2$. For a fixed detector pair at azimuthal angle ψ the time dependence is still given by the angular frequency ω due to the two symmetric lobes of the “figure of eight”. From [11, 24].

219 a signal for the normalized annihilation rate $N_{ij}(t)$ in the form

$$N_{ij}(t) = 1 + a_{ij} \cos(\omega t + \delta_0) + b_{ij} \sin(\omega t + \delta_0), \quad (6.45)$$

220 where t denotes the time the e^+ traverses counter T_0 and δ_0 an instrumental phase common
 221 to all time spectra. The events are contained in a time window of 39.5 ns total width, corre-
 222 sponding to two periods of the accelerator RF. The Fourier coefficients a_{ij} and b_{ij} contain the
 223 complete information of the transverse positron polarization. The analyzing power for anni-
 224 hilation in flight is large in most of the kinematic regions of the experiment. Figure 6.5 shows,
 225 as an example, the contour lines for the transverse analyzing power A_x (in %) as a function
 226 of the sum $u = (E_3 + E_4)/m_e$ and the difference $v = (E_3 - E_4)/m_e$ of the normalized photon
 227 energies E_3 and E_4 .

228 Due to the finite acceptance solid angle for events, the rate of ANN events also varies with
 229 the frequency ω because of a small muon spin rotation (μ SR) decay asymmetry modulated
 230 by the precessing $P_\mu(t)$. By adding or subtracting the Fourier coefficients of appropriate pairs
 231 ij and $i'j'$, it was possible to derive either the μ SR - or the P_T signal, respectively. The μ SR
 232 signal is essential for the experiment, as it allows the decomposition of the vector P_T into its
 233 components (P_{T_1}, P_{T_2}) , since P_{T_1} lies in the plane of k_{e^+} and $P_\mu(t)$ and P_{T_2} perpendicular to
 234 that plane (see Figure 6.1).

235 Table 6.1 shows the results of the general and of a restricted analysis [23]. The average
 236 polarization components $\langle P_{T_1} \rangle$ and $\langle P_{T_2} \rangle$ have been calculated from the values of η, η'' , and
 237 $\alpha'/A, \beta'/A$, respectively. Based on the most general 4-fermion contact interaction (“general
 238 analysis”) the parameter η is given by [12]

$$\eta = \frac{1}{2} \text{Re} \{ g_{LL}^V g_{RR}^{S*} + g_{RR}^V g_{LL}^{S*} + g_{LR}^V (g_{RL}^{S*} + 6g_{RL}^{T*}) + g_{RL}^V (g_{LR}^{S*} + 6g_{LR}^{T*}) \} \quad (6.46)$$

239 With $g_{LL}^V \approx 1$, and all other $g_{\epsilon\mu}^\gamma \approx 0$ [7], one can simplify (6.46) considerably by neglecting all
 240 terms quadratic in non-standard couplings. This amounts to assuming one additional coupling

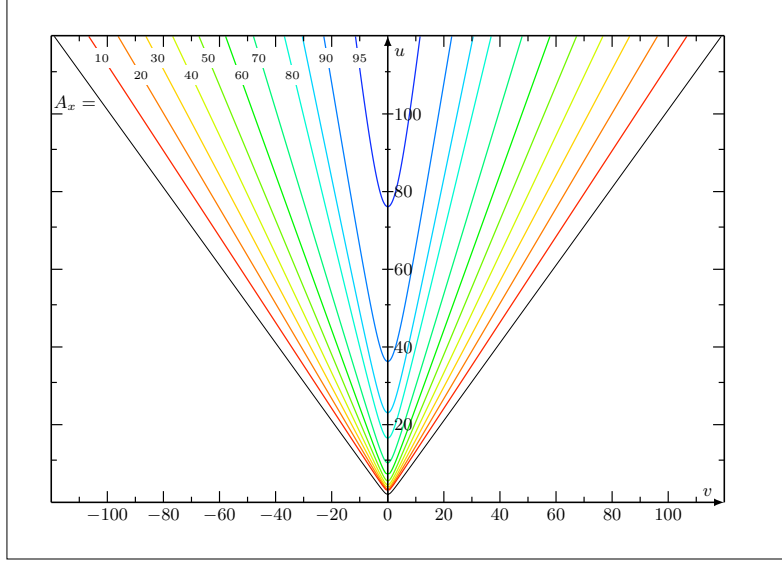


Figure 6.5: Contour lines for the transverse analyzing power A_x (in %) as a function of the sum $u = (E_3 + E_4)/m_e$ and the difference $v = (E_3 - E_4)/m_e$ of the normalized photon energies E_3 and E_4 . The outermost line is the kinematic boundary. From [11].

241 beyond $V - A$. Then only two independent parameters remain ("restricted analysis"):

$$\eta = \frac{1}{2} \text{Re}\{g_{RR}^S\}, \quad \beta'/A = -\frac{1}{4} \text{Im}\{g_{RR}^S\} \quad (6.47)$$

242 Here, g_{RR}^S is a scalar coupling with right-handed μ and e .

243 The Fermi coupling constant G_F is generally derived assuming an exclusive $V - A$ interac-
244 tion, which amounts to setting $\eta = 0$. However, G_F depends on η [2, 12]:

$$G_F \approx G_F^{V-A} \cdot \left(1 - 2\eta \frac{m_e}{m_\mu}\right), \quad (6.48)$$

245 where m_e/m_μ is the mass ratio of electron and muon. Taking η into account increases the
246 relative error $\Delta G_F/G_F$ from 9×10^{-6} to 360×10^{-6} (general analysis) resp. to 68×10^{-6}
247 (restricted analysis).

248 Note that the results on α'/A , β'/A (and deduced from these, $\langle P_{T_2} \rangle$ and $\text{Im}\{g_{RR}^S\}$) are the
249 only experimental data sensitive to the violation of time reversal invariance (TRI) for a purely
250 leptonic *reaction*. In contrast to the violation of TRI in the neutral kaon system [26], a T -
251 odd observable in muon decay would be due to an interference between two couplings with
252 different phase angles and thus be an unambiguous signal of new physics beyond the Standard
253 Model.

254 6.5.3 Electron Decay Asymmetry

255 The measurement of the electron decay asymmetry, $\mathcal{A}(x)$, from polarized muons [27], deter-
256 mines how strongly the chiral components (L, R) of the muon take part in the interaction. This
257 has been used to search for right-handed currents and other muon decay modes outside the
258 Standard Model.

259 If the combination

$$\begin{aligned} \frac{1}{18}(9 + 3\xi - 16 \cdot \xi \cdot \delta) &= \frac{1}{4}|g_{RR}^S|^2 + \frac{1}{4}|g_{LR}^S|^2 + |g_{RR}^V|^2 + |g_{LR}^V|^2 + 3|g_{LR}^T|^2 \\ &\equiv Q_{RR} + Q_{LR} \equiv Q_R^\mu \end{aligned} \quad (6.49)$$

	$V-A$	General analysis	Restricted analysis
η	0	$71 \pm 37 \pm 5$	$-2.1 \pm 7.0 \pm 1.0$
η''	0	$105 \pm 52 \pm 6$	$\equiv -\eta$
α'/A	0	$-3.4 \pm 21.3 \pm 4.9$	$\equiv 0$
β'/A	0	$-0.5 \pm 7.8 \pm 1.8$	$-1.3 \pm 3.5 \pm 0.6$
$\rho_{\eta\eta''}$		946	—
$\rho_{\alpha'\beta'}$		-893	—
$\chi^2/\text{d.o.f.}$		46.2/33	50.3/35
$\text{Re}\{g_{RR}^S\}$	0	—	$-4.2 \pm 14.0 \pm 2.0$
$\text{Im}\{g_{RR}^S\}$	0	—	$5.2 \pm 14.0 \pm 2.4$
$\langle P_{T_1} \rangle$	-3	$6.3 \pm 7.7 \pm 3.4$	
$\langle P_{T_2} \rangle$	0	$-3.7 \pm 7.7 \pm 3.4$	

Table 6.1: $V-A$ values and experimental results. All values, except $\chi^2/\text{d.o.f.}$, in units of 10^{-3} . The correlation coefficients ρ_{ij} are all compatible with zero except the two coefficients listed. The errors are statistical and systematic.

260 has a value different from zero, then a coupling to the right-handed component of the muon
 261 has to exist, i.e. at least one $g_{eR}^\gamma \neq 0$. Conversely, if $Q_R^\mu = 0$, then the coupling acts exclusively
 262 on the left-handed muon.

263 The distribution of the flight direction of the positrons (electrons) is given by (6.5) with
 264 $P_e = 0$ as

$$\frac{d^2\Gamma}{dx d\cos\vartheta} \equiv w(x, \vartheta) \sim \{F_{IS}(x) \pm P_\mu \cos\vartheta F_{AS}(x)\} \quad (6.50)$$

265 This depends on the reduced energy, x , the angle ϑ between the muon polarization and the
 266 positron momentum as chosen by the detector, and on the degree of polarization $P_\mu > 0$. The
 267 asymmetry

$$\mathcal{A}(x) \equiv \frac{w(x, 0) - w(x, \pi)}{w(x, 0) + w(x, \pi)} = P_\mu \cdot \frac{F_{IS}(x)}{F_{AS}(x)} \quad (6.51)$$

268 depends on the parameters ϱ , η , ξ and $\xi\delta$ (see (6.13a), (6.13b), (6.14a) and (6.14b)).

269 The distributions of the flight directions of the positrons (electrons) as seen by an apparatus
 270 that is equally sensitive to positrons of all energies is given by

$$\begin{aligned} \frac{d\Gamma}{d\cos\vartheta} &\sim \int_{x_0}^1 dx \cdot \sqrt{x^2 - x_0^2} \cdot F_{IS}(x) \pm P_\mu \cos\vartheta \cdot \int_{x_0}^1 dx \cdot \sqrt{x^2 - x_0^2} \cdot F_{AS}(x) \\ &\sim (1 \pm \mathcal{A}' \cdot \cos\vartheta) \end{aligned} \quad (6.52)$$

271 The integral asymmetry, \mathcal{A}' , is proportional to $P_\mu \cdot \xi$ and depends on η in first order and on δ
 272 in second order of x_0 . Neglecting x_0 ($x_0 = 0$) one obtains

$$\mathcal{A}' = \frac{1}{3} \cdot P_\mu \cdot \xi \quad (6.53)$$

273 This allows the determination of ξ from an experiment using muons of known polarization.
 274 In the analysis, the knowledge of the values of other muon decay parameters is unimportant.

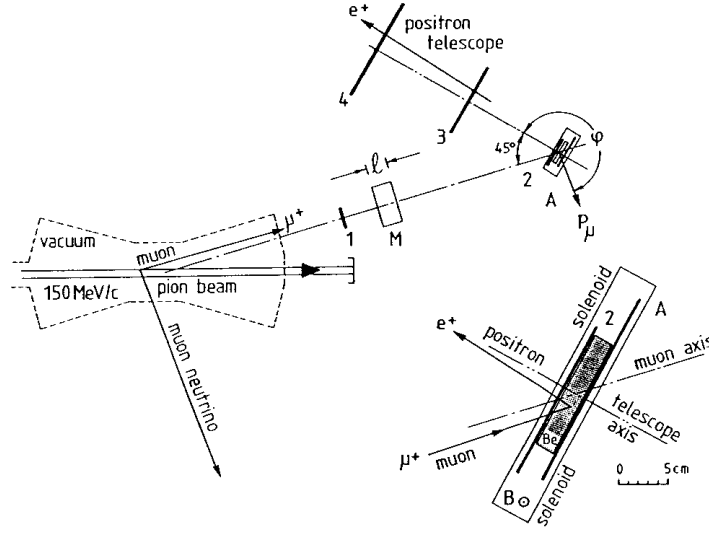


Figure 6.6: Muon Spin Rotation apparatus used to measure the integral asymmetry of the e^+ direction distribution following the decay of highly polarized muons. A parallel beam of monoenergetic ($150 \text{ MeV}/c$) pions decays in flight in vacuum. Muons with energies within a well-determined interval are selected to stop in a beryllium plate, Be, employing a moderator of length ℓ . The original orientation of the muon polarization vector P_μ is thus defined. A rectangular solenoid produces a vertical magnetic field $B = 3 \text{ mT}$ causing the polarization of the stopped muons to precess in the horizontal plane. This gives rise to a sinusoidal modulation of the exponential decrease of the positron rate. The amplitude of the modulation ($\approx 1/3$) is proportional to the quantity desired, $P_\mu \xi$. From [27].

275 Muon beams produced from pions decaying in flight in vacuum avoid Coulomb multiple
 276 scattering. The muon spin lies in the plane of the laboratory line of flight of the original pion,
 277 \mathbf{k}_π , and its decay muon, \mathbf{k}_μ . It points inwards (towards \mathbf{k}_π) for μ^+ and outwards for μ^-
 278 (see Figure 6.6). The transverse and longitudinal muon spin components, ζ_T and ζ_L with
 279 respect to the muon's laboratory line-of-flight are simply given by

$$\zeta_T = \frac{\sin \vartheta_\mu}{\sin \Theta_\mu}, \quad \zeta_L = \mp \sqrt{1 - \zeta_T^2}, \quad (6.54)$$

280 where the upper (lower) sign applies for the muon emitted with smaller (larger) momentum
 281 for the given angle of emission ϑ_μ , and where

$$\begin{aligned} \vartheta_\mu &= \text{laboratory angle between } \mathbf{k}_\pi \text{ and } \mathbf{k}_\mu \\ \Theta_\mu &= \text{maximum laboratory angle by kinematics (Jacobian peak angle)} \\ \sin \Theta_\mu &= (m_\pi^2 + m_\mu^2) / (2m_\pi k_\pi) \\ k_\pi &= \text{pion beam momentum.} \end{aligned}$$

282 The selection of a small slice of muon energy in the laboratory in the vicinity of the Jacobian
 283 peak corresponds to a choice of a small range of neutrino directions and thus of a degree of
 284 polarization $P_\mu = G \cdot P_{\nu_\mu}$. The geometrical factor G , which also has been studied experimentally
 285 [28], is close to one (> 0.99), and it is known with an uncertainty of $< 10^{-3}$ [27].

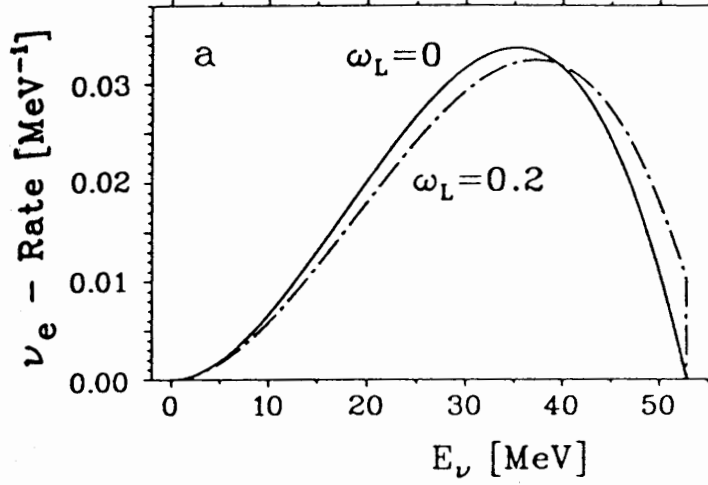


Figure 6.7: Normalized energy distributions of left-handed ν_e from the decay of unpolarized μ^+ . The spectrum shape parameter ω_L is the analog of the Michel parameter ρ of the e^+ . For a pure $V-A$ interaction ω_L is equal to zero. From [33].

286 To measure the decay asymmetry, the muons are stopped in a metal (Be, Al) immersed in
 287 a transverse magnetic field where the spins precess. Detectors track the muon and the decay
 288 positron momenta. The positron intensity has a time modulation corresponding to the decay
 289 asymmetry. It is fortunate that there are substances (Al, Cu, Ag, Au, bromoform) that barely
 290 influence the spin direction of muons inside them. The disappearance of muon polarization
 291 during slowing down [21, 29] and thermalisation [30], i.e. at earlier times compared to the
 292 muon precession time, mimics a smaller \mathcal{A}_{exp} . Depolarization at later times is seen in the data
 293 [31, 32]. It can be accounted for by extrapolating the precession signal amplitude to time zero.
 294 The determination of the extrapolating-function parameters in the same experiment generally
 295 considerably reduces the statistical significance of the data due to their strong correlation with
 296 the signal. The relaxation time in pure metals at room temperature is often conveniently large
 297 compared to the muon lifetime.

298 Positron detectors with low energy thresholds are used for the measurement of $P_\mu \xi$. The
 299 result obtained from this experiment is [27]

$$P_\mu^\pi \xi = (1002.7 \pm 7.9_{\text{stat.}} \pm 3.0_{\text{syst.}}) \times 10^{-3} \quad (6.55)$$

300 As ξ is not limited close to the measured value of $P_\mu \xi$, we cannot draw any specific conclusion
 301 on P_μ and ξ separately. In fact, $-3 \leq \xi \leq +3$. To isolate ξ from $P_\mu \xi$, one has to deduce P_μ
 302 from the measurement of $P_\mu \xi \delta / \rho$ of [32].

303 6.6 Results for τ -lepton and neutrino physics

304 For muon decay, we have shown that a hamiltonian with parity-odd and -even terms is not well
 305 suited for the description of a fully parity-violating interaction. Thus we have extended the
 306 concept of the *chiral* hamiltonian to leptonic τ decays [34]. Assuming universality for leptonic
 307 τ decays sensitivities for the different τ decay constants can be derived.

308 For the complete determination of the interaction in muon decay, it was essential to have
 309 experimental proof that the helicity of left-handed ν_μ is equal to -1 . Previous measurements
 310 had yielded $h_{\bar{\nu}_\mu} = (+990 \pm 160) \times 10^{-3}$ [35] and $h_{\nu_\mu} = (-1060 \pm 110) \times 10^{-3}$ [36]. It was then

311 realized that the measurement of $P_\mu \xi \delta / \varrho$ in muon decay by Carr et al. [37] not only yields
 312 a new lower limit for a possible right-handed W_R boson, but is also suited to derive a vastly
 313 improved limit for the helicity of the ν_μ [38]:

314 The normalized positron rate $d^2\Gamma/dx d\cos\vartheta$ at the spectrum end point can be written as

$$\frac{d^2\Gamma}{dx d\cos\vartheta} = (1 + P_\mu \cdot (\xi \delta / \varrho) \cdot \cos\vartheta) \quad (6.56)$$

315 It is obvious that the factor $|P_\mu \xi \delta / \varrho| \leq 1$, since the rate cannot be negative. P_μ is the polar-
 316 ization of the muon from the decay $\pi^+ \rightarrow \mu^+ \nu_\mu$ and independent of the muon decay constant.
 317 Therefore we find

$$|P_\mu| \leq 1 \quad \text{and} \quad |\xi \delta / \varrho| \leq 1 \quad (6.57)$$

318 On the other hand, from the measurement one gets a lower limit for the product [37]

$$P_\mu \xi \delta / \varrho > 995.9 \times 10^{-3} \quad (90\% \text{CL}) \quad (6.58)$$

319 Since $P_\mu = -h_{\nu_\mu}$ we derive a lower limit for $|h_{\nu_\mu}|$ [38]:

$$|P_\mu| = |h_{\nu_\mu}| > 995.9 \times 10^{-3} \quad (90\% \text{CL}) \quad (6.59)$$

320 It has also been realized that experiments that detect the ν_e from the decay of unpolarized
 321 μ^+ by the reaction $^{12}\text{C}(\nu_e, e^-)^{12}\text{N}(\text{g.s.})$ not only determine the neutrino absorption cross sec-
 322 tion but also measure the ν_e energy spectrum [33]. The energy spectrum can be described by
 323 the spectrum shape parameters ω_L and η_L for left-handed and ω_R and η_R for right-handed
 324 ν_e . In contrast to the energy spectrum of the electrons it allows a new null-test of the standard
 325 model [33]. The right-handed ν_e cannot be detected as they are sterile in matter. For the
 326 energy spectrum of the left-handed ν_e one obtains

$$\frac{d\Gamma_L}{dy} = \frac{m_\mu^5 G_F^2}{16\pi^3} \cdot Q_L^{\nu_e} \cdot \{F_1(y) + \omega_L \cdot F_2(y) + \eta_L x_0 F_3(y)\} \quad (6.60)$$

327 Here, $d\Gamma/dy$ is the probability of a left-handed ν_e to be emitted with the reduced energy
 328 $y = 2E_\nu/m_\mu$. The functions $F_1(y)$, $F_2(y)$ and $F_3(y)$ are given in [33]. The probability $Q_L^{\nu_e}$ of
 329 the ν_e to be left-handed, the spectral shape parameter ω_L and the low energy parameter η_L
 330 are

$$Q_L^{\nu_e} = \frac{1}{4}|g_{RL}^S|^2 + \frac{1}{4}|g_{RR}^S|^2 + |g_{LL}^V|^2 + |g_{LR}^V|^2 + 3|g_{RL}^T|^2 = \frac{1}{2}(1 - P_{\nu_e}) \quad (6.61)$$

$$\omega_L = \frac{3}{4} \frac{\{|g_{RR}^S|^2 + 4|g_{LR}^V|^2 + |g_{RL}^S + 2g_{RL}^T|^2\}}{\{|g_{RL}^S|^2 + |g_{RR}^S|^2 + 4|g_{LL}^V|^2 + 4|g_{LR}^V|^2 + 12|g_{RL}^T|^2\}} \quad (6.62)$$

$$\eta_L = 2 \frac{\text{Re}\{g_{LL}^V g_{RR}^{S*} + g_{LR}^V (g_{RL}^{S*} + 6g_{RL}^{T*})\}}{\{|g_{RL}^S|^2 + |g_{RR}^S|^2 + 4|g_{LL}^V|^2 + 4|g_{LR}^V|^2 + 12|g_{RL}^T|^2\}}, \quad (6.63)$$

331 where P_{ν_e} denotes the longitudinal polarization of the ν_e .

332 References

333 [1] L. Michel, *Interaction between four half spin particles and the decay of the μ meson*, Proc.
 334 Phys. Soc. **A63**, 514 (1950).

- 335 [2] F. Scheck, *Muon physics*, Phys. Rept. **44**, 187 (1978).
- 336 [3] T. Kinoshita and A. Sirlin, *Polarization of electrons in muon decay with general parity*
337 *nonconserving interactions*, Phys. Rev. **108**, 844 (1957).
- 338 [4] M. Fierz, Z. Physik **101**, 553 (1937).
- 339 [5] F. Scheck, *Leptons, Hadrons and Nuclei*, North-Holland, Amsterdam (1983).
- 340 [6] K. Mursula and F. Scheck, *Analysis of leptonic charged weak interactions*, Nucl. Phys.
341 **B253**, 189 (1985).
- 342 [7] W. Fetscher, H. J. Gerber and K. F. Johnson, *Muon decay: Complete determination of the*
343 *interaction and comparison with the standard model*, Phys. Lett. **B173**, 102 (1986).
- 344 [8] F. Scheck, *Electroweak and strong interactions: An introduction to theoretical particle*
345 *physics*, Springer, Berlin (1996).
- 346 [9] C. Bouchiat and L. Michel, *Theory of μ -meson decay with the hypothesis of nonconserving*
347 *of parity*, Phys. Rev. **106**, 170 (1957).
- 348 [10] T. Kinoshita and A. Sirlin, *Muon decay with parity nonconserving interactions and radiative*
349 *corrections in the two-component theory*, Phys. Rev. **107**, 593 (1957).
- 350 [11] W. Fetscher, *Annihilation-in-flight of polarised positrons with polarised electrons as an*
351 *analyser of the positron polarisation from muon decay*, Eur. Phys. J. C **52**, 1 (2007),
352 doi:[10.1140/epjc/s10052-007-0384-6](https://doi.org/10.1140/epjc/s10052-007-0384-6).
- 353 [12] W. Fetscher and H. J. Gerber, in *Precision Tests of the Standard Electroweak Model*,
354 chap. *Precision Tests in Muon and Tau Decays*, pp. 657–705, ed. P. Langacker, World
355 Scientific, Singapore (1995).
- 356 [13] H. Burkard *et al.*, *Muon decay: Measurement of the transverse positron polarization and*
357 *general analysis*, Phys. Lett. **B160**, 343 (1985).
- 358 [14] H. Burkard *et al.*, *Muon decay: Measurement of the positron polarization and implications*
359 *for the spectrum shape parameter eta, ν -a and t invariance*, Phys. Lett. **B150**, 242 (1985).
- 360 [15] H.-J. Gerber, *Lepton properties*, International Europhysics Conference on High Energy
361 Physics (1987).
- 362 [16] C. Jarlskog, Nucl. Phys. **75**, 659 (1966).
- 363 [17] S. Mishra *et al.*, *Inverse Muon Decay, $\nu_{\mu}e \rightarrow \mu^{-}\nu_e$, at the Fermilab Tevatron*, Phys. Lett. B
364 **252**, 170 (1990), doi:[10.1016/0370-2693\(90\)91099-W](https://doi.org/10.1016/0370-2693(90)91099-W).
- 365 [18] D. Geiregat *et al.*, *A New measurement of the cross-section of the inverse muon decay*
366 *reaction muon-neutrino $e^{-} \rightarrow \mu^{-}$ electron-neutrino*, Phys. Lett. B **247**, 131 (1990),
367 doi:[10.1016/0370-2693\(90\)91061-F](https://doi.org/10.1016/0370-2693(90)91061-F).
- 368 [19] H. Toelhoek, Rev. Mod. Phys. **28**, 277 (1956).
- 369 [20] J. DeRaad, Lester L. and Y. J. Ng, *Electron Electron Scattering. 3. Helicity*
370 *Cross-Sections for electron Electron Scattering*, Phys. Rev. D **11**, 1586 (1975),
371 doi:[10.1103/PhysRevD.11.1586](https://doi.org/10.1103/PhysRevD.11.1586).
- 372 [21] G. Ford and C. Mullin, *Scattering of Polarized Dirac Particles on Electrons*, Phys. Rev. **108**,
373 477 (1957), doi:[10.1103/PhysRev.108.477](https://doi.org/10.1103/PhysRev.108.477).

- 374 [22] R. Prieels *et al.*, *Measurement of the parameter ξ'' in polarized muon decay and implications*
375 *on exotic couplings of the leptonic weak interaction*, Phys. Rev. D **90**(11), 112003 (2014),
376 doi:[10.1103/PhysRevD.90.112003](https://doi.org/10.1103/PhysRevD.90.112003), [1408.1472](https://arxiv.org/abs/1408.1472).
- 377 [23] N. Danneberg *et al.*, *Muon decay: Measurement of the transverse polarization of the decay*
378 *positrons and its implications for the Fermi coupling constant and time reversal invariance*,
379 Phys. Rev. Lett. **94**, 021802 (2005), doi:[10.1103/PhysRevLett.94.021802](https://doi.org/10.1103/PhysRevLett.94.021802).
- 380 [24] F. Corriveau *et al.*, *Does the positron from muon decay have transverse polarization?*, Phys.
381 Lett. **B129**, 260 (1983).
- 382 [25] I. C. Barnett *et al.*, *An apparatus for the measurement of the transverse polarization of*
383 *positrons from the decay of polarized muons*, Nucl. Instrum. Meth. **A455**, 329 (2000).
- 384 [26] A. Angelopoulos *et al.*, *First direct observation of time-reversal non-invariance in the neu-*
385 *tral kaon system*, Phys. Lett. **B444**, 43 (1998).
- 386 [27] I. Beltrami, H. Burkard, R. Von Dincklage, W. Fetscher, H. Gerber, K. Johnson, E. Pe-
387 droni, M. Salzmann and F. Scheck, *Muon Decay: Measurement of the Integral Asymmetry*
388 *Parameter*, Phys. Lett. B **194**, 326 (1987), doi:[10.1016/0370-2693\(87\)90552-1](https://doi.org/10.1016/0370-2693(87)90552-1).
- 389 [28] I. Beltrami *et al.*, *Measurement of the integral asymmetry in mu decay and implication for*
390 *the wino mass*, Helv. Phys. Acta **60**, 611 (1987).
- 391 [29] J. Heintze, Z. Physik p. 560 (1957).
- 392 [30] F. G. J.H. Brewer, K.M. Crowe and A. Schenck, *Muon Physics*, vol. III, Academic, New
393 York (1975).
- 394 [31] D. Stoker *et al.*, *Search for Right-handed Currents Using Muon Spin Rotation*, Phys. Rev.
395 Lett. **54**, 1887 (1985), doi:[10.1103/PhysRevLett.54.1887](https://doi.org/10.1103/PhysRevLett.54.1887).
- 396 [32] A. Jodidio *et al.*, *Search for Right-Handed Currents in Muon Decay*, Phys. Rev. D **34**, 1967
397 (1986), doi:[10.1103/PhysRevD.34.1967](https://doi.org/10.1103/PhysRevD.34.1967), [Erratum: Phys.Rev.D 37, 237 (1988)].
- 398 [33] W. Fetscher, *Muon decay: Measurement of the energy spectrum of the electron-neutrino*
399 *as a novel precision test for the Standard Model*, Phys. Rev. Lett. **69**, 2758 (1992),
400 doi:[10.1103/PhysRevLett.69.2758](https://doi.org/10.1103/PhysRevLett.69.2758), [Erratum: Phys.Rev.Lett. 71, 2511 (1993)].
- 401 [34] W. Fetscher, *Leptonic tau decays: How to determine the Lorentz structure of the*
402 *charged leptonic weak interaction by experiment*, Phys. Rev. D **42**, 1544 (1990),
403 doi:[10.1103/PhysRevD.42.1544](https://doi.org/10.1103/PhysRevD.42.1544).
- 404 [35] R. Abela, G. Backenstoss, W. Kunold, L. Simons and R. Metzner, *Measurements of the*
405 *polarization of the 2P and 1S states in muonic atoms and the helicity of the muon in pion*
406 *decay*, Nucl. Phys. A **395**, 413 (1983), doi:[10.1016/0375-9474\(83\)90051-9](https://doi.org/10.1016/0375-9474(83)90051-9).
- 407 [36] L. Roesch, V. Telegdi, P. Truttmann, A. Zehnder, L. Grenacs and L. Palffy, *Measurement of*
408 *the average and longitudinal recoil polarizations in the reaction C-12 (μ^- , neutrino) B-12*
409 *(G.S.): pseudoscalar coupling and neutrino helicity*, Helv. Phys. Acta **55**, 74 (1982).
- 410 [37] J. Carr *et al.*, *Search for Right-Handed Currents in Muon Decay*, Phys. Rev. Lett. **51**, 627
411 (1983), doi:[10.1103/PhysRevLett.51.627](https://doi.org/10.1103/PhysRevLett.51.627), [Erratum: Phys.Rev.Lett. 51, 1222 (1983)].
- 412 [38] W. Fetscher, *Helicity of the muon-neutrino in π^+ decay: a comment on the measurement of*
413 *$P(MU) XI DELTA / RHO$ in muon decay*, Phys. Lett. B **140**, 117 (1984), doi:[10.1016/0370-](https://doi.org/10.1016/0370-2693(84)91059-1)
414 [2693\(84\)91059-1](https://doi.org/10.1016/0370-2693(84)91059-1).